THE PUBLISHING HOUSE
OF THE ROMANIAN ACADEMY

PROCEEDINGS OF THE ROMANIAN ACADEMY, Series A,
Volume 22, Number 3/2021, pp. 235–243

DESIGN OF A MAGNETIC SPRING FOR VARIABLE STIFFNESS ACTUATORS

Radu OLARU, Camelia PETRESCU, Alexandru ARCIRE

"Gheorghe Asachi" Technical University of Iasi, Faculty of Electrical Engineering, Iasi, Romania
Corresponding author: Radu OLARU, E-mail: rolaru@tuiasi.ro

Abstract. This paper describes a novel, innovative magnetic spring having the stiffness depending on the current in the coil(s), designed to be used in applications where an adjustable/controllable stiffness is needed, for example in variable stiffness actuators (VSAs) or in controllable vibration dampers. The device has in principal two magnets in repulsive disposition, one or two coils and a particular magnetic structure. The results from simulation and optimization of a reference model of controllable stiffness magnetic spring (CSMS) with one coil led to the design and construction of a prototype of CSMS with two coils which were studied experimentally. The comparative analysis of the device operation, with control current only in the main coil and then in both inserted coils, led to the conclusion that the secondary coil contributes to an important increase of the CSMS performance. Thus, for example, for a control current varying between –2A and +2A, the range of variation of the elastic forces, the maximum range of variation of the stiffness, and the level of control for the stiffness, can be doubled. The main advantage of the proposed CSMS is the ability to vary in the simplest and most direct way the stiffness and force of the magnetic spring, which ensures speed and dynamics in controlling the operation of CSMS-based systems.

Key words: magnetic spring, controllable stiffness, variable stiffness actuator (VSA), variable stiffness.

1. INTRODUCTION

Magnetic springs began to develop after the appearance of high performance magnets based on Nd-Fe-B alloys. While the conventional mechanic springs impose some limitations on the system regarding mainly compactness, friction, material fatigue and failure, magnetic springs show potential to overcome these issues especially for short strokes and frequent operation. Thus, research in recent years shows that magnetic springs based on repulsive or attractive permanent magnets can be an alternative to mechanical springs in many technical applications e.g. semi-active vibration isolations and suspensions [1, 2], energy harvesters from vibration [3, 4], oscillatory drives [5, 6, 7], vibration generators or shakers [8, 9]. The main arrangements of magnetic springs encountered in the mentioned applications are: simple spring with two repulsive magnets, differential spring with three repulsive magnets, and repelling-attraction combination spring.

Many current modern devices and systems require the use of adjustable and controllable elastic elements, such as: variable stiffness actuators (VSAs), active vibration dampers, vibro-insulating platforms and robots. For example, VSAs are devices for gripping manipulated objects or for joints in compliant and dexterous robots. A variable stiffness actuator, in contrast to a stiff actuator, allows deviations from its own equilibrium position, depending on an external force [10]. In principal, VSAs have an adaptable compliance mechanism in addition to elastic elements storing energy and altering the stiffness. Two motors are required: one to control the equilibrium position and the second to control stiffness [11]. The elasticity of VSAs is given by the elasticity of the springs used.

At the same time, controlled stiffness magnetic springs could present a challenge for the improvement and modernization of VSAs, by replacing the mechanical elastic systems with the electromagnetic ones based on magnetic springs, simpler and easier to control, especially useful in highly dynamic applications.

Very few papers found in technical literature have so far dealt with magnetic springs with controllable stiffness. We found only three papers that address the variable stiffness actuation with magnetic springs. A variable stiffness gripper with antagonistic magnetic springs is described in [12]. The robot gripper consists

of two parallel fingers where repulsive magnets are used as nonlinear springs between gripper actuators and fingers. Position and rigidity of the fingers are simultaneously controlled by adjusting the air-gap between magnets. The application of the proposed gripper is discussed for dynamic manipulation, where the variable stiffness is exploited to improve the performance of a hammering task. In [13] a MAVERIC device is reported, containing a variable stiffness coupler that can be used as a clutch, with a variable stiffness magnetic torsion spring, which may be used as an elastic element for the VSAs. The device contains two co-axial diametrically magnetized hollow cylinders and has two degrees of freedom: a rotation of the two cylinders around the common axis and a relative translation along the same axis. The stiffness of the equivalent torsion spring can be varied continuously from a maximum value down to zero by changing the axial overlap of the two cylinders.

In both cases presented above, the change in stiffness is done with external mechanical actions (servomotors) on the magnetic spring which determine either the change of the compression of the magnetic springs, or the change of the axial position of two magnetized cylinders.

A controlled magnetic spring which can be applied in a vibration reduction system of the machine operator seat is described in [14]. The magnetic spring consists of two stationary magnets and two mobile magnets. The magnetic circuit has a magnetic core that is configured with four magnetic poles on which four coils are fixed, an upper magnetic core and a lower magnetic core. The force depends on the current sign and amplitude and on the number of active coils. The switching of the current in the four coils allows a force variation between 444 and 733 N. It should be mentioned that the magnetic spring control is done discontinuously and the variation of magnetic spring stiffness is between relatively low limits, as can be deduced from the analysis of the force vs. displacement curves.

In this paper an original controllable magnetic spring is developed, where the force and stiffness of the magnetic spring can be varied easily, continuously and rapidly with a command current.

2. SIMULATION STUDY OF A CONTROLLABLE STIFFNESS MAGNETIC SPRING

Figure 1 illustrates the concept of Controllable Stiffness Magnetic Spring (CSMS), where the stiffness of the magnetic spring can be modified by a control current. The two magnets are associated with a coil and a magnetic structure consisting of housing, carcass, three pole pieces and a ring [15]. The magnetic structure ensures the direction of the magnetic flux produced by the coil fed with current in the air gap between the two magnets. The magnetic flux of the coil is superimposed over the magnetic flux of the two magnets and, depending on the direction of the current in the coil, a higher or lower total magnetic flux is obtained than in the absence of electric current. The result is an increase or decrease of the magnetic spring force, respectively, accompanied by a change in its stiffness, as will be shown below. The + and – signs in the figure signify the direction of the current through the coil, $+I$ and $-I$, respectively, for an I current, that determines the increase or decrease of the total magnetic flux of the electromagnetic assembly, i.e. the increase or decrease of the magnetic spring force.

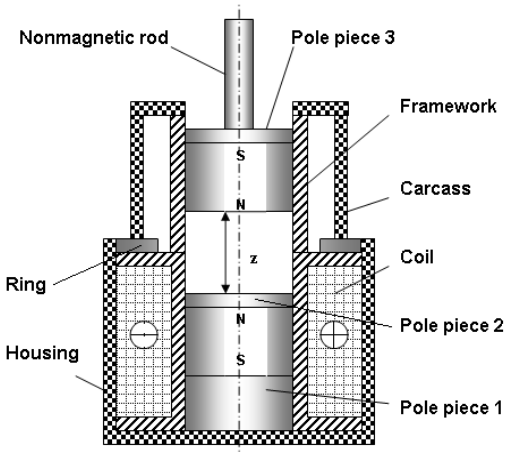

Fig. 1 – Conceptual model of CSMS used in simulation study.

The model used in simulation has the dimensions outlined in Table 1. The magnets have the diameter and height of 15mm and 8mm, respectively. The inner diameter and height of the coil are 18 mm and 22 mm, respectively. The coil has $N = 450$ copper wires, 0.55 mm in diameter.

Due to the model symmetry, a 2D simulation was performed for magnetic field analysis and force calculation, using the AC/DC module in the COMSOL 5.3 software.

Table 1

Dimensional values (in mm) for magnetic components in Fig. 1

Carcass outer diameter $d_{ca.o}$	Carcass inner diameter $d_{ca.i}$	Carcass height h_{ca}	Housing outer diameter d_{ho}	Housing inner diameter d_{hi}	Housing height h_h	Pole piece 1, height h_{pp1}	Pole piece 2, height h_{pp2}	Pole piece 3, height h_{pp3}	Ring inner diameter d_{ri}	Ring height h_r
24÷40	20÷36	24	40	36	26	8.5	2	2	24	2

The magnetic spring characteristics $F(z)$ offer the possibility to define some functional parameters of CSMSs that may be necessary for VSA applications. One such parameter is the stiffness coefficient at an operating point, $\left(z_i, F(z_i, I)\right)$, given by the expression,

$$k_i\left(z_i, F(z_i, I)\right) = \left.\frac{\mathrm{d}F(z, I)}{\mathrm{d}z}\right|_{z=z_i}. \tag{1}$$

This parameter can be modified within a wide range by varying the current in the two limits, $-I$ and $+I$.

A qualitative parameter, Level of Stiffness Control, L_{cs} (non-dimensional), is defined with relation (2) as the ratio between the difference of maximum stiffness in two active points of operation located on the curves of maximum positive and maximum negative current, and the stiffness in a point on the passive curve ($I=0$), at equilibrium:

$$L_{cs} = \frac{\Delta k_m}{k_0} = \frac{(k_{1m+} - k_{2m-})}{k_0}. \tag{2}$$

In (2) k_0, k_{1m+} and k_{2m-} represent the stiffness coefficient of the spring in a passive position of the spring $\left(z_0, F_0(z_0, 0)\right)$, in an active position of the spring at positive current $\left(z_1, F_1(z_1, +I)\right)$ and in another active position of the spring at negative current, $\left(z_2, F_2(z_2, -I)\right)$, respectively. Relation (2) can be detailed as in relation (3):

$$L_{cs}(z_0, z_1, z_2, I) = \frac{k_{1m+}\left(z_1, F_1(z_1, +I)\right) - k_{2m-}\left(z_2, F_2(z_2, -I)\right)}{k_0(z_0, 0)} = \frac{\mathrm{d}F_1(z, +I)/\mathrm{d}z\big|_{z=z_1} - \mathrm{d}F_2(z, -I)/\mathrm{d}z\big|_{z=z_2}}{\mathrm{d}F_0(z, 0)/\mathrm{d}z\big|_{z=z_0}}. \tag{3}$$

Changing the stiffness variation of the magnetic spring and the compliant actuator can be separated into two basic interactions with the environment. One is changing stiffness at constant position and the second is changing stiffness at constant load/force [16]. For example, when a robot is changing stiffness at constant position, usually the robot is at a certain position or on a given track and the intention is that the stiffness should be modified without affecting the output position. Rewriting relation (3) for this case, using the same value of the current I in the coil in both directions, leads to the expressions for the level of stiffness control $L_{cs.p}$ at a constant position $z_0 = \text{const.}$:

$$L_{cs.p}(z_0, I) = \frac{k_{1m+}\left(z_0, F_1(z_0, +I)\right) - k_{2m-}\left(z_0, F_2(z_0, -I)\right)}{k_0\left(z_0, F_0(z_0, 0)\right)} = \frac{\mathrm{d}F_1(z, +I)/\mathrm{d}z\big|_{z=z_0} - \mathrm{d}F_2(z, -I)/\mathrm{d}z\big|_{z=z_0}}{\mathrm{d}F_0\left(z_0, F_0(z_0, 0)\right)/\mathrm{d}z\big|_{z=z_0}}. \tag{4}$$

From the analysis of the curves in Fig. 2, for the model without carcass, and the data in Table 2, it results that the magnetic spring force, the stiffness coefficient, the maximum range for k and the control level

increase with the increase of the ring width (decrease of the inner diameter, up to the value d_{ri} = 22 mm), which represents the further adopted value, due to the best output parameters and the shape of the plots. In Table 3, $\Delta k_m = k_{m+} - k_{m-}$, represents the maximum variation of the stiffness coefficient at z = 6 mm, as the difference between the maximum stiffness constant, k_{m+}, corresponding to the maximum current value I_+ and the minimum stiffness constant, k_{m-}, corresponding to the maximum current value I_-.

As may be seen from the analysis of the plots in Fig. 3 and the values of the parameters in Table 3, the presence of the upper magnetic housing leads to an important increase of the stiffness constant k, keeping approximately the value of its maximum range of variation, Δk_m, and also to a relatively small decrease of $L_{cs.p}$. In these conditions, we will choose the upper magnetic housing with the outer diameter equal to 40 mm, the same as that of the bottom housing, having the advantage of constructive simplicity and a single cylindrical housing for the entire device. In addition, as will be seen in chapter 4, this creates the space for using a second coil in the upper part, to increase the CSMS performance.

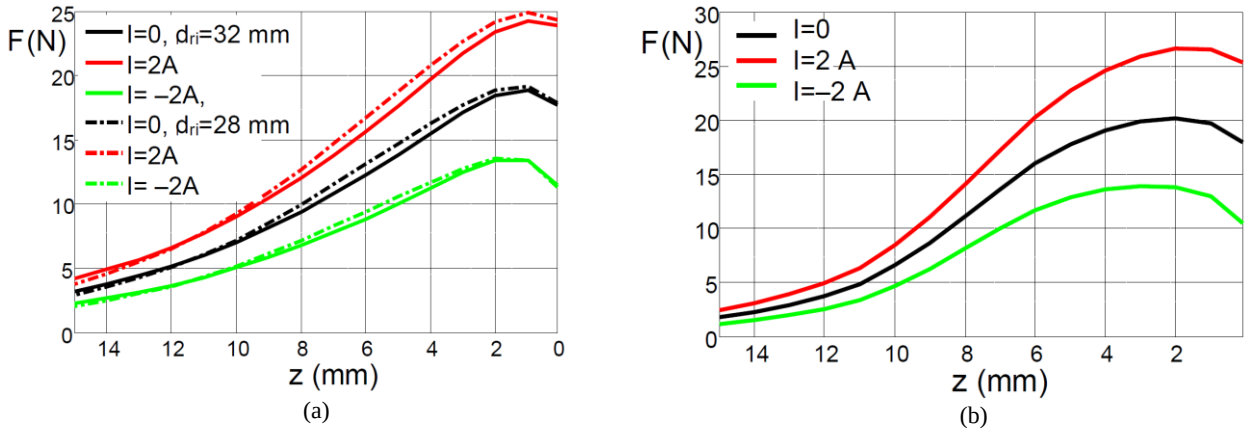

Fig. 2 – Magnetic spring plots for the model in Fig. 1, without carcass, for different values of the inner ring diameter: a) d_{ri} = 32 mm and 28 mm; b) d_{ri} = 22 mm, adopted value.

Table 2

Parameters depending on d_{ri}, for z = 6 mm: k (N/mm), $L_{cs.p}$ (%) and Δk_m (N/mm), for CSMS model without magnetic carcass

d_{ri} (mm)		32	28	24	22
k (N/mm)	I = 0	1.46	1.58	1.86	2.11
	I = +2A	1.86	2.03	2.44	2.77
	I = –2A	1.05	1.11	1.29	1.44
$L_{cs.p}$ (%)		55.5	58.2	61.8	63.0
Δk_m (N/mm) = $k_{m+} - k_{m-}$		0.81	1.08	1.15	1.33

Table 3

Parameter dependence on $d_{ca.o}$, for z = 6 mm: k, $L_{cs.p}$ and Δk_m

$d_{ca.o}$ (mm)		40	36	32	28
k (N/mm)	I = 0	2.21	2.27	2.48	2.46
	I = +2A	2.88	2.94	3.12	3.1
	I = –2A	1.53	1.61	1.82	1.83
$L_{cs.p}$ (%)		61.1	0.59	0.52	0.52
Δk_m (N/mm) = $k_{m+} - k_{m-}$		1.35	1.33	1.3	1.27

An improvement in the shape of the curves in Fig. 3, in order to eliminate the decrease of forces at z < 2 mm is possible by reducing the thickness of polar piece 2. Figure 4 and Table 4 illustrate the curves for the optimized CSMS and its parameter values, respectively, using polar piece 2 with the height reduced to h_{pp2} = 1.5 mm. The improved shape of the curves allows the increase of the operating interval, Δz, with an acceptable nonlinearity, an important increase of $L_{cs.p}$, but also reductions of the parameters k and Δk_m. These parameter reductions represent the price paid for the compromise made regarding the increase of the control performance of the studied device.

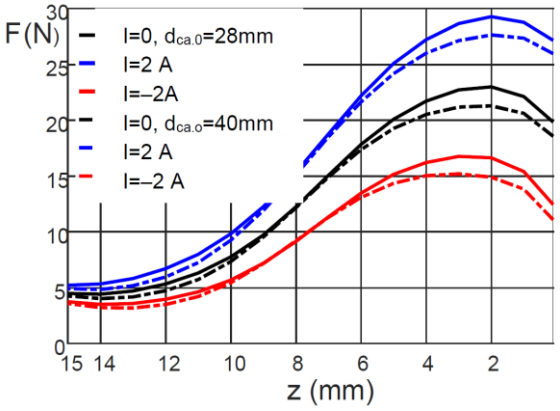

Fig. 3 – Magnetic spring characteristics for the CSMS model with carcass in Fig. 1, having the outer diameter $d_{ca.o}$ = 40 mm and 28 mm, and inner ring diameter d_{ri} = 22 mm.

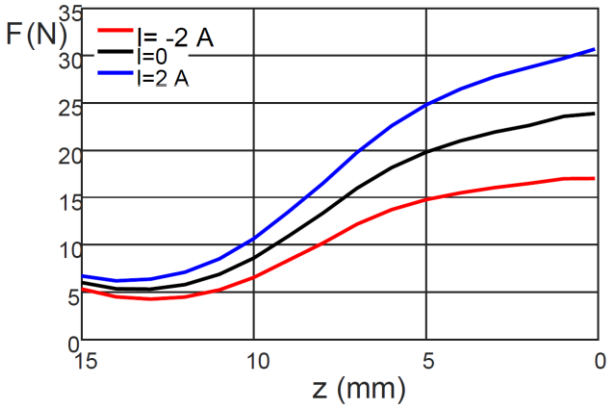

Fig. 4 – Force *vs.* compression curves for optimized CSMS having: polar piece 2 with height, h_{pp2} = 1.5 mm, outer carcass diameter $d_{ca.o}$ = 40 mm and inner ring diameter d_{ri} = 22 mm.

Table 4

Parameters of optimized CSMS for z = 6 mm

I (A)	–2	0	2
k (N/mm)	1.23	1.85	2.5
$L_{cs.p}$ (%)	68,6		
Δk_m (N/mm) = $k_{m+} - k_{m-}$	1.27		

3. VARIABLE STIFFNESS ACTUATORS WITH CSMS

A broad classification of the VSAs has been presented in [11] where the four main classes have been defined regarding the method of stiffness control: equilibrium controlled, antagonistic controlled, structure controlled and mechanically controlled. The antagonistic controlled stiffness method requires two actuators with nonlinear force-displacement characteristic, which are coupled antagonistically to act against each other. Using both devices simultaneously, the equilibrium position and stiffness can be controlled. In this context, we can find several uses of CSMSs in VSAs, of which we mention two:

– a positioning motor and a CSMS (Fig. 5a);

– two antagonistic motors and two antagonistic CSMSs (Fig. 5b).

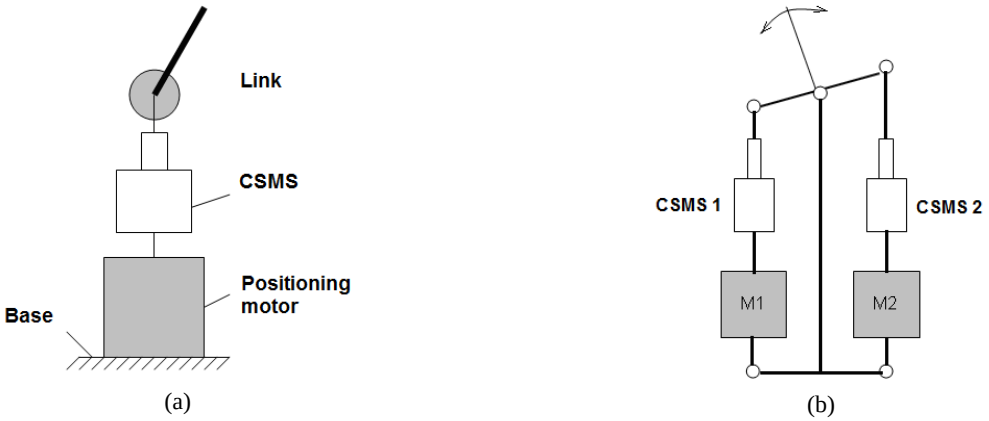

(a) (b)

Fig. 5 – Two VSA principles using CSMSs: a) independent motor setup with one CSMS; b) two antagonistic motors with two antagonistic CSMs.

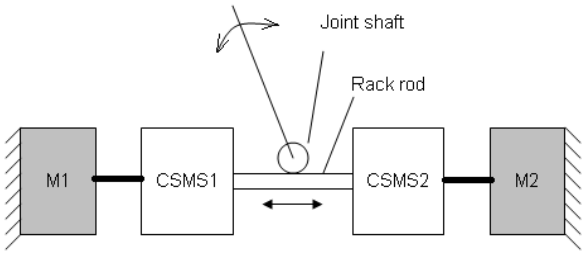

Fig. 6 – Two antagonistic motors with two antagonistic CSMSs arranged in line.

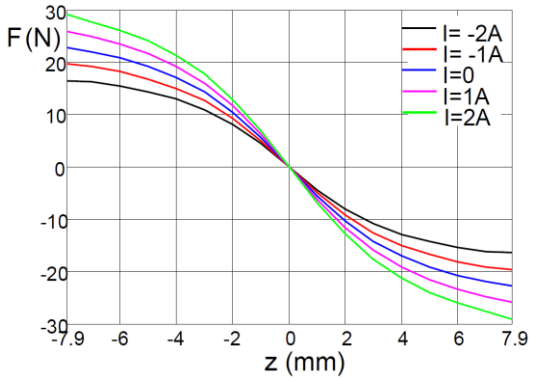

Fig. 7 – Force *vs.* compression curves for two antagonistic CSMSs with spring preload at 8 mm.

Figure 5 shows two variants of series elastic actuator (SEA), where a spring is in series with a stiff actuator. The compliance in SEA is determined by the spring constant and is therefore not adjustable during operation. Using a spring with variable stiffness, such as the CSMS in Figure 5a, allows a mode of operation with variable compliance used to reduce load shocks, for example. The variant with the antagonistic scheme from Figure 5b allows a much more compliant operation. If the application allows, a simpler constructive variant than the one in Figure 5b is the use of two antagonistic motors and two antagonistic CSMSs arranged in line, Figure 6. To change the equilibrium position both motors have to work in the same direction. To change the stiffness both motors have to move in opposite direction to preload the two springs, as is the case in VSAs with mechanical springs. In addition, using CSMSs achieves a wide range of stiffness variation during operation by modifying the control current. At the same time, only a fixed spring preload of the CSMS by the motors and the variation of the stiffness during VSA operation by the two CSMSs can be used.

Figure 7 shows the force vs. compression curves for two antagonistic CSMSs with spring preload at 8 mm, for which the best k values were obtained, Δk_m, $L_{cs.p}$ and α (Table 5). The coefficient $\alpha = \Delta k/\Delta I$ (N/mmA) represents the rate of increase of the CSMS stiffness with the control current, which is determined for the portions of curves with linear variation near the origin of the axes.

Table 5

Parameters k, Δk_m, $L_{cs.p}$ and α for two antagonistic CSMSs with spring preload at $z_0 = 8$ mm

I (A)	–2	–1	0	1	2
k (N/mm)	4.43	5.05	5.67	6.3	6.92
Δk_m (N/mm) = $k_{m+} - k_{m-}$	2.49				
$L_{cs.p}$ (%)	43.9				
α (N/mmA) = $\Delta k/\Delta I$	0.622				

4. EXPERIMENTAL RESULTS

A CSMS prototype was designed and realized practically (Fig. 8), based on the results obtained using numerical simulation, Chapter 3, for the single-coil CSMS model. The device has mainly undergone three changes compared to the studied theoretical and optimized model, which do not produce negative effects, but contribute to a significant increase in the main parameters of the device, such as force, stiffness and level of stiffness control. The three changes consist of using a single, common housing, adding a coil identical to the first one around the mobile magnetic assembly and increasing the winding window to accommodate a number of 600 turns instead of 450, as used in the theoretical study. The two caps each have a thickness of 8 mm, so the dimensions of the prototype are: the diameter of 48 mm and the height of 67 mm (without shaft). The two coils are connected in phase opposition.

The experimental results for plotting the variation curves of the CSMS forces as a function of the z position were obtained using a mechanical measuring assembly illustrated in Fig. 9.

Figure 10 illustrates the *z*-position force variation curves, obtained by simulation and experiment, of the CSMS prototype that uses a single coil. Figure 11 shows the same types of curves but in the case when the CSMS device uses two coils. It is found that while the shape of the experimental curves is very close to that of the curves obtained by simulation, there are deviations of the experimental results from the simulated ones, higher at low values of *z* and in the case of the command with current $I_+ = 2$A. We appreciate that these deviations are due to the significant increase of the magnetic flux density *B* in certain local areas of the ferromagnetic parts of the magnetic circuit, reaching values close to the saturation induction of the magnetic material, which leads to a significant decrease of zonal magnetic permeability and, consequently, to a redistribution of the magnetic flux obtained by simulation and finally, to a decrease of the real magnetic forces compared to those calculated numerically.

Table 6 contains the parameters determined experimentally forming the basis for the comparative evaluation of the two variants of CSMS operation.

As it results from the comparative analysis of the curves in Figs. 10 and 11 and of the data from Table 6, the addition of a supplementary coil contributes to the increase of the variation range of the elastic forces and of the CSMS operation parameters. Thus, if for the current variation from –2A to + 2A in the main coil of the CSMS, we have the variation of the elastic forces between 5 N at $z = 10$ mm and 15 N at $z = 4$ mm, in case of using both coils, the variation of the elastic forces is between 10.5 N and 25 N for the same values $z = 10$ mm and 4 mm, respectively. This means an increase in the range of variation of elastic forces by 67% at $z = 4$ mm to over 100%, practically doubling the range of variation of forces for *z* exceeding 10 mm.

The maximum stiffness variation, Δk_m, and the level of stiffness control, $L_{cs.p}$, increase by the same percentage values when using both coils, respectively by approximately 24% and 127%, for $z = 6$ and 8 mm, respectively.

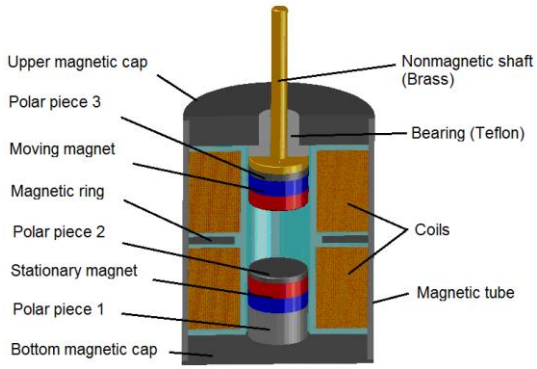

Fig. 8 – Design of CSMS prototype with two coils.

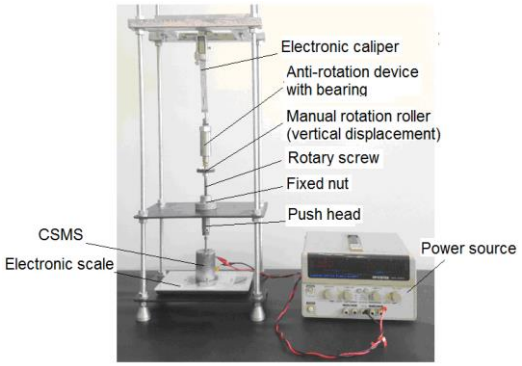

Fig. 9 – Experimental setup.

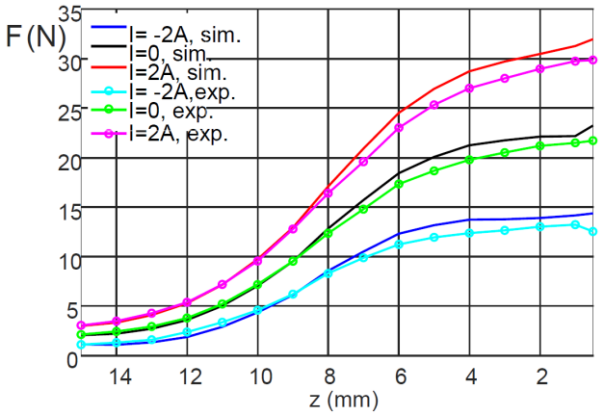

Fig. 10 – Force *vs.* compression curves for CSMS prototype using a single coil.

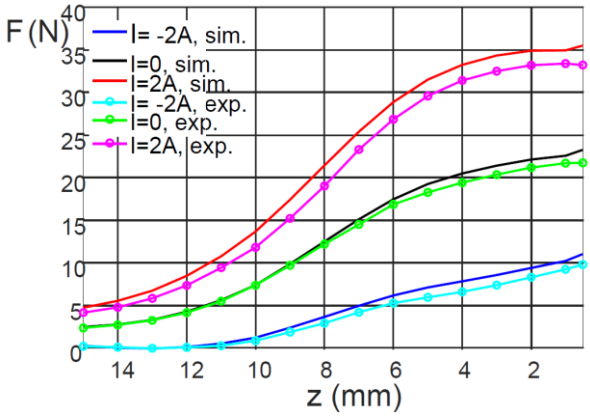

Fig. 11 – Force *vs.* compression curves for CSMS prototype using two coils.

Table 6

Experimental parameters: k, Δk_m and $L_{cs.p}$ at z = 6 and 8 mm for CSMS prototype using one or two coils

		A single coil			Two coils		
I (A)		–2	0	2	–2	0	2
k (N/mm)	z = 6 mm	0.86	1.95	2.71	0.92	1.95	3.22
	z = 8 mm	1.95	2.71	3.54	1.39	2.71	5.01
Δk_m (N/mm) = $k_{m+} - k_{m-}$	z = 6 mm	1.85			2.33		
	z = 8 mm	1.59			3.62		
$L_{cs.p}$ (%)	z = 6 mm	94.9			117.9		
	z = 8 mm	58.7			133.6		

5. CONCLUSIONS

An original controllable magnetic spring useful in designing devices and systems with adjustable compliance was developed and studied theoretically and experimentally. The basic magnetic configuration, the effect of magnetic components and the concept of CSMS were explained and justified using the magnetic spring curves obtained by simulation. In order to assess the performance of a CSMS model, the constant stiffness, k, and several other specific parameters were considered, such as the maximum variation of the stiffness coefficient, Δk_m, and the level of stiffness control, $L_{cs.p}$, the last one being defined in this paper.

A direct search deterministic optimization with respect to several geometric parameters was conducted. The simulation study led to obtaining an optimized reference model of CSMS with one coil, which offers the possibility to design a CSMS according to the application specific requirements, easier and simpler construction, slimmer and small size, than in the variant with two coils. Two VSA principles using CSMSs, similar to the optimized reference model, were presented and discussed: independent motor setup and a CSMS, with two antagonistic motors and two CSMSs. In both cases CSMS ensures adjustable compliance during system operation. For an antagonistic variant with in-line operation of the VSA system, the values of the four parameters taken into account, k, Δk_m, $L_{cs.p}$ and α were obtained and discussed. By changing the spring preload produced with the help of the two servomotors of the VSA system, the range of variation of the operating parameters can increase a lot.

A prototype CSMS with two coils was designed, built and tested experimentally. The effect of using the second coil is analyzed by comparing three parameters obtained from the experimental curves, the stiffness coefficient, k, the maximum variation of stiffness coefficient Δk_m, and the level of stiffness control, $L_{cs.p}$, obtained at CSMS operation with one coil and with two coils, respectively. It was found that the addition of a supplementary coil to the main one contributes to the increase of the variation range of the elastic forces and of the CSMS operation parameters. Thus, at the variation of the control current between –2A and + 2A, the range of variation of the elastic forces, the maximum range of variation of the stiffness, and the level of control for the stiffness, can be doubled.

The experimental results are in a satisfactory agreement with those obtained by numerical simulation, thus demonstrating the functionality and utility of the proposed model of the controlled stiffness magnetic spring.

The new model of magnetic spring with controllable stiffness has a simple construction, low cost, is easily controllable and can have applications in the development of new and original systems of actuators and of vibration control designed to perform actuation, handling and damping operations.

REFERENCES

1. Z.H. ZHOU, S.H. CHEN, D. XIA, J.J. HE, P. ZHANG, *The design of negative stiffness spring for precision vibration isolation using axially magnetized permanent magnet rings*, Journal of Vibration and Control, **25**, *19-20*, pp. 2667-2677, 2019.
2. T. LIXIN, D. HAIPING, D. MINGMING, N. DONGHONG, W. YANG, L. WENXING, *Semiactively controllable vehicle seat suspension system with negative stiffness magnetic spring*, IEEE/ASME Transactions on Mechatronics, **26**, *1*, pp. 156-167, 2021.

3. A. NAMMARI, L. CASKEY, J. NEGRETE, H. BARDAWEEL, *Fabrication and characterization of non-resonant magneto mechanical low-frequency vibration energy harvester*, Mechanical Systems and Signal Processing, **102**, pp. 298-311, 2018.
4. R. OLARU, R. GHERCA, C. PETRESCU, *Analysis and design of a vibration energy harvester using permanent magnets*, Rev. Roum. Sci. Techn. – Électrotechn. et Énerg., **59**, pp. 131-140, 2014.
5. F. POLTSCHAK, P. EBETSHUBER, *Design of integrated magnetic springs for linear oscillatory actuators*, IEEE Transactions on Industry Applications, **54,** pp. 2185-2192, 2018.
6. Z. JIAO, T. WANG, L. YAN, *Design and analysis of linear oscillating motor for linear pump application-magnetic field*, dynamics and thermotics, Front. Mech. Eng., **11**, *4*, pp. 351-362, 2016.
7. P.J. MISLJEN, Ž.V. DESPOTOVIC, M.S. MAJEVIC, *Modeling and control of bulk material on the electromagnetic vibratory feeder*, Automatika, **57**, *4*, pp. 936-947, 2016.
8. R. OLARU, A. ARCIRE, C. PETRESCU, M.M. MIHAI, N.B. GÎRTAN, *A novel vibration actuator based on active magnetic spring*, Sensors and Actuators A: Physical, **264**, *1*, pp. 11-17, 2017.
9. R. OLARU, M.M. MIHAI, B. GÎRTAN, C. PETRESCU, A. ARCIRE, *Design and experiment of an electromagnetic vibrational inertial actuator using linearized magnetic spring*, Rev. Roum. Sci. Techn. – Électrotechn. et Énerg., **63**, *3*, pp. 253-258, 2018.
10. R. VAN HAM, T. SUGAR, B. VANDERBORGHT, K. HOLLANDER, D. LEFEBER, *Compliant actuator designs*, IEEE Robotics & Automation Magazine, **16**, pp. 81-94, 2009.
11. B. VANDERBORGHT, A. ALBU-SCHAFFER, A. BICCHI, E. BURDET, D.G. CALDWELL, R. CARLONI, M. CATALANO, O. EIBERGER, W. FRIEDL, G. GANESH, M. GARABINI, *Variable impedance actuators: A review*, Robotics and Autonomous Systems, **61**, pp. 81-94, 2013.
12. A.H. MEMAR, E.T. ESFAHANI, *A variable stiffness gripper with antagonistic magnetic springs for enhancing manipulation*, In: *Robotics: Science and Systems*, 2018, DOI:10.15607/RSS.2018.XIV.053.
13. A. SUDANO, D. ACCOTO, L. ZOLLO, E. GUGLIELMELLI, *Design, development and scaling analysis of a variable stiffness magnetic torsion spring*, International Journal of Advanced Robotic Systems, **10**, *372*, pp. 1-11, 2013.
14. J. SNAMINA, P. HABEL, *Magnetic spring as the element of vibration reduction system*, Mechanics and Control, **29**, *1*, pp. 40-44, 2010.
15. R. OLARU, C. PETRESCU, *Magnetic spring with controllable elasticity*, Patent pending, OSIM no. A00863, 2018.
16. S. WOLF, G. GRIOLI, O. EIBERGER, W. FRIEDL, M. GREBENSTEIN, H. HOPNER, E. BURDET, D.G. CALDWELL, R. CARLONI, M.G. CATALANO, D. LEFEBER, *Variable stiffness actuators: Review on design and components*, IEEE-ASME Transactions on Mechatronics, **21**, pp. 2418-2430, 2016.

Received January 15, 2021